

ORIGINAL ARTICLE | DOI: 10.5584/jiomics.v3i1.126

Vascular Smooth Muscle Cells activation revealed by quantitative phosphoproteomics analysis

Claudia Boccardi^{1,2,*§}, Vittoria Matafora^{3,4,§}, Giovanni Signore², Silvia Rocchiccioli¹, Maria Giovanna Trivella¹, Emanuele Alpi³, Lorenzo Citti¹, Angela Bachi³, Antonella Cecchetti^{1,5}

[§]These authors contributed equally to this work; ¹Institute of Clinical Physiology, CNR, Pisa, Italy; ²Center for Nanotechnology Innovation @NEST, Istituto Italiano di Tecnologia, Pisa, Italy; ³San Raffaele Scientific Institute, Division of Genetics & Cell Biology, Milan, Italy; ⁴Department of Internal Medicine, Second University of Naples, Naples, Italy; ⁵Clinical and Experimental Medicine, University of Pisa, Pisa, Italy.

Received: 22 January 2013 Accepted: 14 April 2013 Available Online: 10 May 2013

ABSTRACT

Vascular smooth-muscle cells (VSMCs) are the main components of the artery medial layer and if activated by growth factors as a consequence of vessel injuries, acquire the ability to proliferate and migrate contributing to the formation of neointima. In the early phase/events of VSMC stimulation a cascade of kinases and phosphatases initiates phospho-events that are decisive for VSMC activation. In this work, a SILAC approach in a multi-strategy combined method for phosphopeptides enrichment was used, in order to gain insights into the phosphomodulation of the proteome of VSMCs stimulated by platelet derived growth factor BB (PDGF-BB). The quantitative SILAC phosphoproteome analysis allowed the identification of 1300 phosphopeptides among which 47 resulted novel phosphosites. Some important factors involved in cytoskeleton remodeling, focal adhesions, gap junction assembly and cell activation have been found differentially phosphorylated, highlighting their pivotal role in early VSMC reorganization and suggesting a novel starting point to assess the precise actors of VSMC activation and their roles.

Keywords: quantitative phosphoproteomics; SILAC; VSMC activation; PDGF-BB.

1. Introduction

Vascular smooth muscle cells (VSMCs), although highly specialized, are not terminally differentiated cells. They maintain a great plasticity and, when stimulated by external inputs, they are able to switch to an activated phenotype characterized by increased cell proliferation capability and triggering of cell proliferation and migration programs [5,6]. These properties are helpful for vascular healing following injury and damage, but can also be detrimental since they exert, a pivotal role in onset and progression of vascular proliferative disorders contributing to the thickening of the tunica intima, named neointima, and the beginning of the atherosclerotic plaque [7]. A wide range of elements contributes to VSMC activation and, among them, growth factors are the most critical ones. Platelet derived growth factor –BB (PDGF-BB), produced by activated platelets and macrophag-

es, has so far been the only factor demonstrated to selectively and directly promote VSMC phenotype changes [5,8].

Following growth factor binding to its receptor, a cascade of kinases and phosphatases are activated and, within a few minutes, a series of events and specific responses are triggered while the phosphorylation state of the proteins changes dramatically [9]. These early events, even if phenotypically imperceptible, are decisive for the activation process in VSMCs [6, 10], and result with a complete reorganization of the cell structure.

Indeed, several stimuli regulate both VSMC differentiation and activation through phosphorylation [11]. Chen and colleagues in 2010 investigated the signal transduction pathways of heat shock protein 27 (HSP27) phosphorylation in VSMCs after angiotensin II (ANG-II) and PDGF-BB stimu-

*Corresponding author: Claudia Boccardi, Institute of Clinical Physiology, CNR, Pisa, Italy; Phone number: +39050509769; Fax number: +39050509417; E-mail address: claudia.boccardi@iit.it

lation [12]. Similarly, Liu *et al.* observed the promotion of VSMC proliferation via the phosphoinositol-3-kinase/Protein Kinase B (PI3K/Akt) pathway induced by apelin-13 [13]. Recently, in an *in vivo* rat carotid injury model, overexpression of Smad3 produced an increase in phosphorylated extracellular signal-regulated kinases (ERK) mitogen-activated protein kinases (MAPK) as well as increased VSMC proliferation [14].

Several MS-based quantification methods have been exploited for the study of the phosphoproteome [15, 16, 17], highlighting how accuracy and reliability of phosphorylation sites identification and quantitation is of key importance. Among others, stable-isotope labeling of amino acids in cell culture (SILAC) is a simple and straightforward approach [18], which allows the metabolic labeling in living cells and minimizes variations that could be introduced during sample preparation. However, some limitations still remain in a global phosphoproteomics approach, due to the low amount of phosphorylated proteins [19], and these are overcome by the use of phosphopeptide enrichment methods [20,21,22].

In this work, we used SILAC in a multi-strategy combined method for phosphopeptides enrichment in order to gain insights into the phospho-modulation of VSMC proteome stimulated by PDGF-BB. In particular, as the phosphorylation events are really fast and dynamic, we analyzed two different time points after stimulation: 10 minutes and 2 hours. 1300 phosphopeptides, clustering into 380 protein groups were identified. Among them, 21 phosphopeptides (corresponding to 16 proteins) resulted phospho-modulated at different times upon PDGF-BB stimulation. These proteins are involved in cytoskeleton remodeling, focal adhesions, gap junction assembly and cell activation indicating that the events related to PDGF-BB phosphorylation pathway are the triggering phenomena in VSMC activation.

2. Material and methods

2.1 Chemicals, standards and consumables

ACN, water, formic acid used for LC-MS analysis were from Fluka, Sigma Aldrich St. Louis, MO; sequencing grade trypsin was purchased from Promega (Madison, WI). SILACTM DMEM medium, fetal bovine serum (FBS), L-lysine, L-arginine, [13C6]-L-Lysine and [13C6]-L Arginine were purchased from Invitrogen (USA, CA). [U-13C6, U-15N2] Lysine and [U-13C6,U-15N4] Arginine were purchased at CIL (USA). Recombinant Human PDGF-BB was from R&D (USA). Coomassie Plus protein assay was from Pierce, Bio-Spin Column from Biorad and PHOS-Select Iron Affinity Gel (IMAC resin) was purchased from Sigma Aldrich. All other chemicals were purchased from Sigma Aldrich.

2.2 Cell Culture and SILAC-Labeling

SILACTM D-MEM medium containing 2 mM L-

Glutamine, 10% dialyzed FBS, and 100 U/mL penicillin and streptomycin was supplemented with 100 mg/L L-lysine and 100 mg/L L-arginine; 100 mg/L [¹³C6]-L-Lysine and 100 mg/L [¹³C6]-L Arginine or 100 mg/L [U-¹³C6, U-¹⁵N2] Lysine and 100 mg/L [U-¹³C6,U-¹⁵N4] Arginine to prepare the “Light” (L), “Medium” (M) or “Heavy” (H) SILAC culture media, respectively. VSMCs were obtained from coronaries of 8-month-old domestic crossbred pigs (*Sus scrofa domestica*) and the investigation was conformed to Ministerial Decree to authorize testing n.06/2009-b. Cells isolation was performed according to the method described by Christen *et al.* [23] and VSMCs were expanded in SILAC medium for 6 doublings to ensure nearly 100% incorporation of labeled amino acids. For the experiments three biological replicates (cells isolated from at least three different pieces of coronary coming from three different animals) and then pooled before analysis. Prior to cell treatment, all “heavy”, “medium” and “light” cells were cultured overnight in their corresponding SILAC media without FBS. For PDGF-treatment, medium labeled cells (M) were treated for 10 minutes (t10min) with 100 ng/mL of PDGF-BB; heavy labeled cells (H) were stimulated for 2 hours (t2h) with PDGF-BB while Light labeled cells (L) were not treated with the growth factor (t0).

2.3 Protein lysate preparation and in-solution digestion

VSMCs were harvested with trypsin and lysed in 50mM Tris-HCl pH 8, 0.25% sodium deoxycholate, 0.5% Triton X100, 10mM sodium orthovanadate, 5mM sodium fluoride. For each of three specimens (L, M and H cells), three million cells were re-suspended in 400 µl of lysis buffer. After 30 min in ice, samples were sonicated and then centrifuged at 10000xg for 30 min at 4 °C to produce a clarified lysate. L, M and H VSMC lysates were mixed at 1:1:1 [w/w] ratio, the protein amount was determined by Coomassie Plus protein assay. In total, 9 mg of the 1:1:1 mixed protein lysate was precipitated with a standard chloroform/methanol precipitation protocol. Precipitated proteins were re-suspended in 450 µl of 100 mM Tris-HCl pH 8.

Disulfide bonds were reduced with 5 mM DTT for 60 min at room temperature, and then the free sulfhydryl groups were alkylated with 10 mM iodoacetamide at room temperature in the dark for 30 min. Protein digestion was performed using a total of 18 µg of sequencing grade trypsin with 15 h incubation at 37°C.

2.4 Strong Cation Exchange (SCX) Chromatography

Preparative separations were carried out with SCX resin, using Bio-Spin Microcolumns. The first equilibration resin step was carried out using 4.5 mL of solution A (5 mM KH₂PO₄, pH 2.65; 30% ACN; 0,1% TFA) for 5 min. Then 4.5 mL of regeneration buffer were used (5mM KH₂PO₄, 30% ACN, 0.1% TFA, 1M KCl, pH 2.7). The first step was repeated. The peptide mixtures were diluted with 4.5 mL of SCX

solution A and placed on the resin at room temperature for 40 minutes. Increasing concentrations of solution B (5mM KH_2PO_4 , 30% ACN, 0.1% TFA, 350mM KCl, pH 2.7) from 5% to 100% in 7 steps (5, 10, 15, 20, 25, 50, 100) were used to elute peptides.

2.5 Immobilized Metal-Affinity Chromatography (IMAC)

PHOS-Select Iron Affinity Gel was used for IMAC fractionation using the same microcolumn. As first step, resin was washed three times with 200 μL of binding solution (0.1% TFA, 30% ACN). 50 μL of PHOS-Select slurry were added to each SCX fraction. After 60-min incubation at room temperature with vigorous shaking, the supernatant was removed (IMAC flow-through). The resin was washed with 200 μL of binding solution and added to IMAC flow-through. The mono-phosphorylated peptides and non-phosphorylated peptides were eluted from IMAC resin using acidic conditions (200 μL of 1% TFA, 20% ACN), while the poly-phosphorylated peptides were subsequently eluted from the same IMAC resin using ammonium hydroxide (200 μL of NH_4OH pH 11.2). After concentration (from 1mL to 0.1mL) in dry vacuum the pooled flow-through was further analyzed by TiO_2 chromatography. The mono-phosphorylated peptide fraction was also subjected to TiO_2 chromatography as described below. Basic elution samples were submitted to LC-MS/MS analysis directly.

2.6 Titanium Dioxide (TiO_2) Chromatography

Samples were diluted nine times with TiO_2 binding solution (5mg/mL DHB, 80% ACN and 3% TFA). 160 mg of TiO_2 resin were re-suspended in 1.4 mL of TiO_2 binding solution. 200 μL of TiO_2 resin slurry were added to each sample for 30 min at room temperature. The supernatant was removed by centrifugation in a microcolumn. Non-specific binders were removed by two washes with 500 μL of 50% ACN, 0.2% TFA solution. Phosphopeptides bound were eluted from TiO_2 micro-columns using 200 μL of ammonium hydroxide, 40% ACN pH 12.5 followed by 100 μL of 100% ACN.

2.7 Mass Spectrometry

Mass spectrometry analysis was performed on a LTQ-Orbitrap mass spectrometer (Thermo Scientific, Bremen, Germany). Tryptic digests for each sample were cleaned using Stage Tips as described previously [24] and then injected in a capillary chromatographic system (EasyLC, Proxeon Biosystems, Denmark); Peptide separation occurred on a homemade column obtained with a 10-cm fused silica capillary (75 μm inner diameter and 360 μm outer diameter; Proxeon Biosystems) filled with 3 μm resin Reprosil-Pur C18 (Dr. Maisch GmbH, Ammerbuch-Entringen, Germany) using a pressurized "packing bomb". A gradient of eluents A (distilled water with 2% (v/v) ACN, 0.1% (v/v) formic acid)

and B (2% (v/v) ACN, distilled water with 0.1% (v/v) formic acid) was used to achieve separation from 8% B (at 0 min, 0.2 μL -min flow rate) to 50% B (at 80 min, 0.2 μL -min flow rate). The LC system was connected to the Orbitrap equipped with a nanoelectrospray ion source (Proxeon Biosystems). Full-scan mass spectra were acquired in the mass range m/z 350 to 1500 Th and with the multistage activation enabled for neutral loss of phosphoric acid [32.66, 48.99, and 97.97 atomic mass units (amu)][25]. All full-scan spectra were recalibrated in real time with the lock-mass option [26]. The 5 most intense doubly and triply charged ions were automatically selected and fragmented in the ion trap.

2.8 Data analysis

The raw MS data were processed and analyzed using MaxQuant software version 1.0.13.13. The required FDR was set to 0.01 at both the peptide and protein level and the minimum required peptide length was set six amino acids. The MS/MS spectra were searched against Uniprot mammalia 2010_07 database supplemented by frequently observed contaminants, concatenated with reversed versions of all sequences. Mascot (version 2.2.07) was used for the database search. Enzyme specificity was set to trypsin, additionally allowing up to two missed cleavages. The search included cysteine carbamidomethylation as fixed modification and N-acetylation of protein, oxidation of methionine, and phosphorylation of serine, threonine and tyrosine as variable modifications. Protein SILAC ratios are reported as the median of the ratios derived from SILAC triplets assigned to the protein. For phosphopeptides, the phosphorylation site(s) were assigned with a modified version of the PTM score [27] given in MaxQuant. MaxQuant automatically quantified SILAC peptides and proteins. SILAC protein ratios were calculated as the median of all peptide ratios assigned to the protein. Ratio Variability was less than 30%. Systematic deviations, such as mixing errors, were corrected by the quantitation algorithm in the MaxQuant software by normalizing all peptide ratios such that the mean of all log-transformed ratios were zero. A posterior error probability for each MS/MS spectrum below or equal to 0.1 was required. In case the identified peptides of two proteins were the same or the identified peptides of one protein included all peptides of another protein, these proteins (e.g. isoforms and homologs) were combined and reported as one protein group. Phosphorylation sites were made non-redundant with regards to their surrounding peptide sequence. Nevertheless all alternative proteins that matched a particular phosphosite were reported as one group. The PTM score was used for assignment of the phosphorylation site(s) as described [27]. To match identifications across different replicates and adjacent fractions, the "match between runs" option in MaxQuant was enabled within a time window of 5 min.

2.9 Bioinformatics analysis

We based the annotation of proteins on Uniprot identifiers. Pathway membership information was obtained from the KEGG database (<http://www.genome.jp/kegg/pathway.html>). Phospho_ELM BLAST Search PhosphoSite (<http://phospho.elm.eu.org/pELMBlastSearch.html>) database was used to retrieve known phosphorylated sites and relative kinases.

2.10 SILAC incorporation

For incorporation test, a small aliquot of cells was lysed using the above mentioned protocol. Briefly, 10µg of total lysate were loaded on SDS-PAGE. A section of the gel was digested with trypsin, and peptides were purified on StageTips and analyzed with a single LC-MS/MS run. Raw files were processed by MaxQuant analysis to determine the ratio of heavy labeled peptides to the remaining unlabeled

ones. The calculation for lysine- and arginine-containing peptides was performed separately. The probability density function analysis was obtained by kernel density estimation (KDE) using the R software package (ver. 2.10.1) (Figure 1–Supplementary data).

3. Results and Discussion

3.1 Workflow: description and assessment

In this study, we performed SILAC experiments to quantify changes in phosphorylation upon PDGF-BB stimulus. The schematic experimental workflow is depicted in Figure 1. One advantage of SILAC is that it allows the combination of differentially labeled protein samples early during sample preparation. This is especially important for the experiments related to this study because several sample fractionation and enrichment steps were involved. Our method combines SILAC for phosphopeptide quantitation, SCX fractionation,

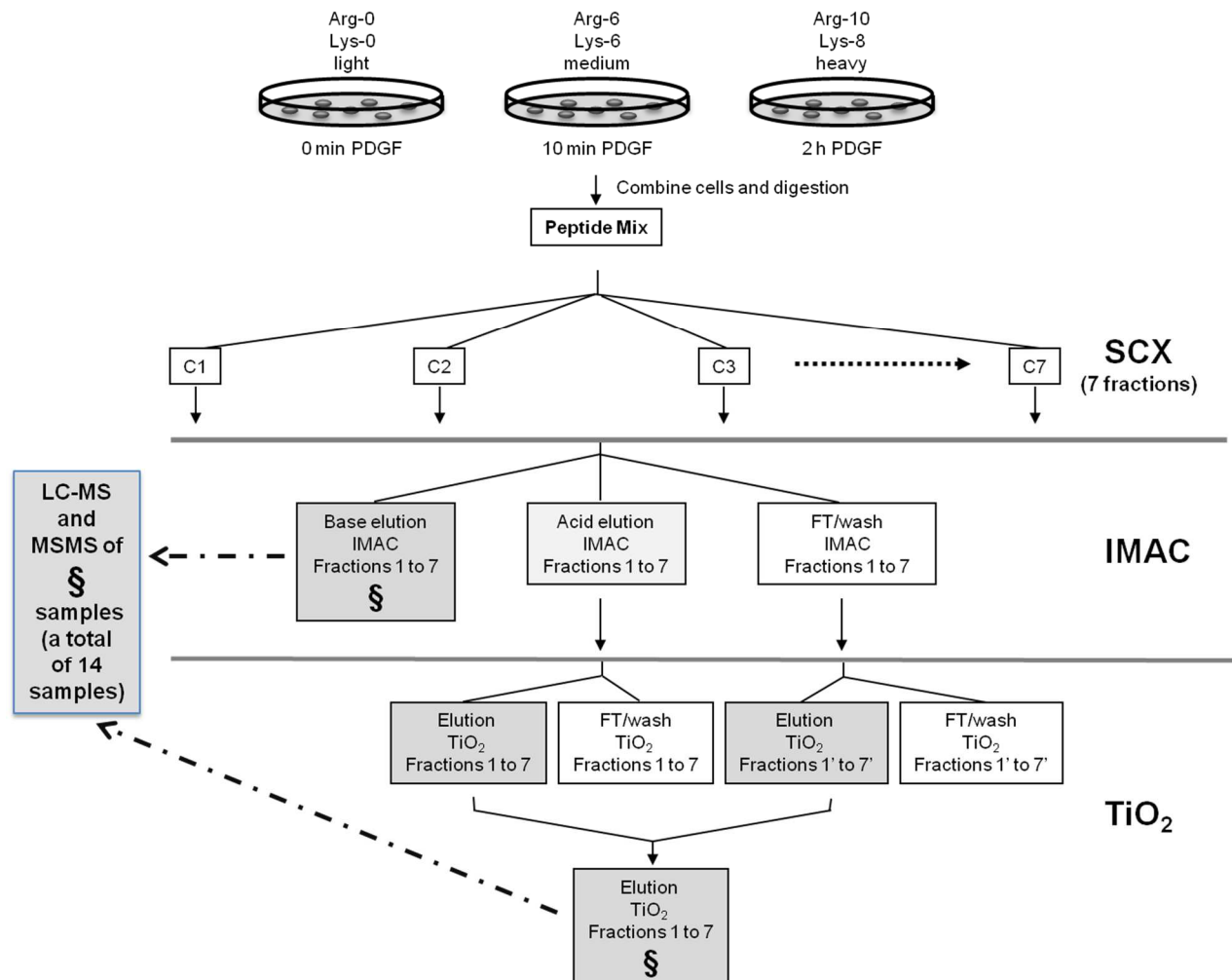


Figure 1. Schematic workflow representation. Primary VSMCs, were cultured and stimulated with PDGF-BB at different time and different SILAC medium (L for t0; M for t10min and H for t2h). Protein extracts were mixed 1:1:1 and enzymatically in solution digested. The resulting peptide mixtures were separated into 7 fractions by SCX fractionation. Every fraction was enriched for phosphopeptides using first IMAC and then, TiO₂ beads. Only the 14 different sample fractions obtained after IMAC (7 fractions) and after TiO₂ (7 fractions) were analyzed by LC-MS/MS (fractions marked with \$). Two technical LC-MS/MS replicates were examined for each fraction.

sequential elution from IMAC (SIMAC) [28] and multi-stage LC-MS to obtain a highly accurate phospho selection and identification. Primary VSMCs, obtained from pig coronary arteries, were cultured and stimulated with PDGF-BB (100 ng/mL) for 10 minutes and 2 hours and labeled with both arginine and lysine using three distinct isotope forms (L for t0, M for t10min and H for t2h). Protein extracts were mixed 1:1:1 and enzymatically digested in solution. The resulting peptide mixtures were separated into 7 fractions by SCX [29] and phosphopeptides enriched by IMAC [30, 31]. Every fraction was enriched in phosphopeptides using first IMAC and then, TiO₂ beads.

Only the 14 different fractions obtained after IMAC (7 fractions, see figure 1) and after TiO₂ (7 fractions, see figure 1) were analyzed by LC-MS/MS, to specifically identify phospho-peptides and proteins. Two replicates of each fraction were examined by online liquid chromatography on a linear ion trap/Orbitrap mass spectrometer. Each peptide was eluted as characteristic triplets: one peptide unlabeled for t0 and the other two peptides differently labeled on arginine or lysine for the two different PDGF-BB stimulation times (t10min and t2h). The intensity of each component of triplet reflects the relative amounts at the three time points

chosen. Technical reproducibility of SILAC quantification for each peptide was proved to be really excellent ($R^2 > 0.93$) (Figure 2-Supplementary data).

Comparing results in terms of phosphopeptides identification, TiO₂ selection enable the identification of 86% of the total phosphopeptides, with only 12% overlapping with IMAC selection (Figure 2A).

Considering that the SILAC approach was applied for the first time to VSMC model to quantitatively analyze time-course modifications, we evaluated the level of labeled amino acid incorporation in these primary cells and the possible cellular morphological changes induced by the treatments. Labeling efficiency, calculated separately for lysine- and for arginine-containing peptides, was very high, above 96% for both labeled samples (M and H) (Figure 1, panel A Supplementary data) demonstrating both the feasibility of SILAC quantitation in primary VSMCs and the precision of the experiment (Figure 1, panel B Supplementary data). Moreover, confocal microscope images obtained staining VSMCs with the specific marker α -SM-actin showed no differences in cell morphology and/or marker distribution in cells grown in the three SILAC media compared to those cultured in standard conditions (data not shown).

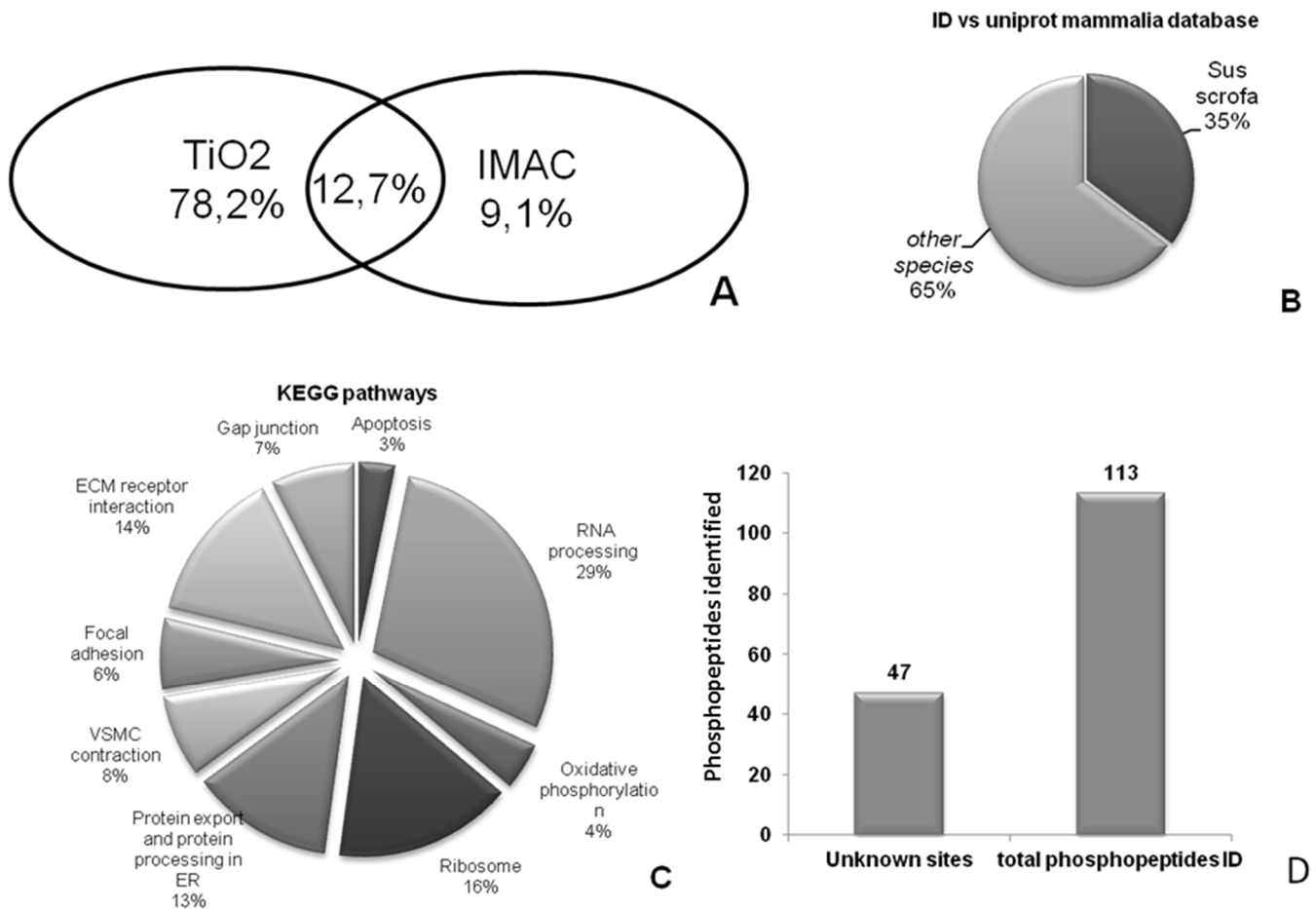


Figure 2. Characterization of identified proteins. A: Venn diagram compares the number of phosphorylated peptides identified in TiO₂ and IMAC fractions. B: percentage of peptides identified in *Sus scrofa* dataset. C: KEGG pathway analysis. D: analysis of total non-redundant identified phosphopeptides.

Table 1. Differentially phosphorylated peptides. Proteins corresponding to the peptides are reported in the first column. The numbers of phosphorylation sites, the putative amino-acidic phosphorylated residues, the enzymes likely involved in the phosphorylations are indicated. The columns tagged as 10min and 2h quote the phosphorylation trend at 10 minutes or 2 hours after stimulation (▲; up-regulated, ▼; down-regulated). The last two columns report the information on the known phosphorylation site.

Protein Name	KEGG Pathway	N°P-sites (STY)	AA Probable Phospho (STY)	10'	2h	Known site	Best Motif
Calreticulin	Protein processing in ER	1	Y FY(1)GDQEKDK	▲			
Gap junction alpha-1 protein (Connexin 43)	Gap junction	1	S KLDAGHELQPLAIVDQRPS(0.926)R	▲			CAMK2
Gap junction alpha-1 protein (Connexin 43)	Gap junction	1	S ASS(0.988)RPRPDDLEI	▲		Known site	CAMK2
Gap junction alpha-1 protein (Connexin 43)	Gap junction	1	S AS(0.5)SRPRPDDLEI	▲			PKA
60S acidic ribosomal protein P2	Ribosome	1	S KEESEES(1)DDDMGFGLFD	▲	▲	Known site	CK1
60S acidic ribosomal protein P2	Ribosome	1	S KEES(1)EESDDDMGFGLFD	▲	▲		
High mobility group protein HMG-I/HMG-Y		1	S KLEKEEEEGISQES(0.9)SEEEQ	▲	▲	Known site	CK2
High mobility group protein HMG-I/HMG-Y		2	S KLEKEEEEGISQES(0.998)S(0.998)EEEQ	▲	▲	Known site	CK2
HSP27		1	S QLSSGVS(0.73)EIQTADR		▲	Known site	CK1
Caldesmon	VSMC contraction	1	S QSVDKVTS(0.967)PTKV		▲		
Filamin A		1	S APS(1)VANVGSHCDLSLK	▼			PKA/AKT
PDZ and LIM domain protein 5		1	S SPS(0.746)WQRPNQAAAPSTGR	▼			
Vinculin	Focal adhesion	1	S DPTAS(1)PGDAGEQAIR	▼			
MCG7378;Sec61 beta subunit; translocation complex beta variant	Protein processing in endoplasmic ER	1	S PGTPSGTNVGSSGRS(0.949)PSK	▼		Known site	CDK2
Nucleophosmin		1	S LLSIS(1)GK	▼		Known site	NEK6
Aa2-041;BCL2-associated transcription factor 1, isoform CRA_a		1	Y Y(0.414)SPSQNSPIHHIPSR	▼	▼	Known site	
Coiled-coil domain-containing protein 67		1	S VLYQTHLVSLDAQKLLS(0.99)EK	▼	▼		GSK3
Collapsin response mediator protein 4 long variant		1	S GS(0.986)PTRPNPPVR	▼	▼	Known site	DYRK2
Collapsin response mediator protein 4 long variant		1	T GSPT(0.777)RPNPPVR	▼	▼		CDK2
EPLIN-b		1	S LENEETLERPAQLPNAAEIPQS(1)PGVEDAPIAK	▼	▼		WGroupIV
Ybx1 protein;Nuclease-sensitive element-binding protein 1		1	S NYQQNYQNSE(0.598)GEKNEGSESAPEGQAQQR	▼	▼	Known site	

3.2 Phosphoproteome analysis of PBGF-BB stimulated VSMCs

Quantitation of phosphorylation sites was obtained via MaxQuant analysis [32]. A total of 42 LC-MS/MS analyses allowed the identification of a total of 1300 phosphopeptides distributed on 380 protein groups (see Supplementary Table 1 and 2). Although satisfactory, these data are underestimated owing to the partial completion of the *Sus scrofa* database [33]. In order to compensate this shortcoming we used the Uniprot cp mammalia database to identify not only phosphopeptides belonging to *Sus scrofa* but also phosphorylated peptides highly homologous in other mammalian species

(Figure 2B).

Phospho_ELM BLAST Search PhosphoSite was used to look for novel, still unidentified, phosphorylated sites. Among the non-redundant 113 phosphorylated sites identified, 42% (corresponding to 47 new phosphorylation sites) were not yet previously reported in Mouse-Human database (identified through sequence homology between Pig and Mouse-Human) (see Supplementary Table 1 and Figure 2D). For the phospho-modulated proteins, more than 50% of the sites were identified as new in the Mouse-Human database.

It is worth noting that all identified phosphorylation sites are not present in the *Sus Scrofa* database highlighting the great drawback of using pig as a model organism. Notwith-

standing, pig remains an important animal model for cardiovascular disease experimentations and thus it could be valuable to annotate the database with our findings.

Using 1.7 fold as SILAC ratio cutoff (corresponding to $P < 0.05$ as calculated by MaxQuant significance B and using the ratio M/L and H/L normalized by MaxQuant on median intensity), we found 21 phosphopeptides statistically modulated at different times of stimulation (Table 1, Figure 3). Ten of them (belonging to 6 different proteins) were up-regulated, while the remaining eleven (belonging to 10 different proteins) resulted to be down-regulated upon PDGF-BB stimulation at both time points.

One potential concern for quantitative phosphoproteomics is that changes in protein expression can affect phosphopeptide/phosphoprotein ratios. In our SILAC analyses, for each replicate, we used the same cell population under the same growing conditions. At the last passage, cells were subdivided in three groups, all of them cultured for 24h without serum and afterwards two parts were treated with PDGF-BB as indicated while the thirdset of cells was left untreated. The time of treatment was short and thus we reasoned that it would not lead to significant changes in protein expression. This hypothesis was also confirmed from the analysis of the ratio M/L and H/L of the entire proteome identified (Figure 3 and 4-Supplementary data.) Before harvesting, cells were counted in order to use in the successive analyses the same number of them for each treatment.

KEGG pathway analysis of the identified phosphoproteins revealed that phosphorylation events in the activation process induced by PDGF-BB are involved in several functions including RNA and protein processing, extra cellular matrix (ECM)-receptor interaction, VSMC contraction, gap junction regulation and oxidative phosphorylation (Figure 2C).

Phosphoproteomic changes after PDGF stimulus

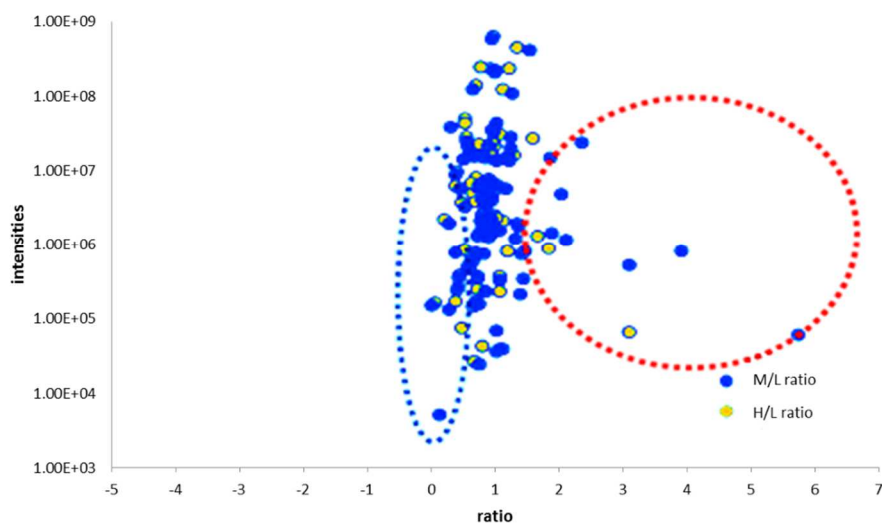


Figure 3. Quantitative phosphoproteomic analysis of PBGF-BB stimulated VSMCs. Scatter plot of the ratios M/L or H/L versus intensities of the identified phosphopeptides. Up-regulated phosphopeptides are grouped in the red circle, while in the blue circle the down-regulated ones are highlighted.

The most represented functions (RNA and protein processing) are related to transcription and translation activities. This last observation is interesting since the early events (from 10 min to 2h of growth factor stimulation) are initial stages towards the acquisition of the activated, synthetic phenotype which extensively engaged in new proteins synthesis.

Finally, it is interesting, the analysis of the kinases potentially involved in the activation process induced by PDGF-BB. Figure 4 shows the results of phosphopeptides that were predicted to be associated with kinase binding motif by SCANSITE. The computer algorithm SCANSITE was used to predict the kinase substrate relationship from dataset. The panel A shows the known motif distribution for all identified phosphorylation sites. The panel B shows instead the same analysis restricted for the sites of modulated proteins in our “in vitro” cardiovascular pathogenesis model. The analysis of the most frequent protein kinase related with the phosphomodulated proteins were normalized in order to better analyze the frequency of phosphorylation motif in our system. (Figure 4 panel C)

It is interesting to note that Ca²⁺/calmodulin-dependent protein kinases 2 (CAMK2), cyclin-dependent kinase 2 (CDK2) and casein kinase 1 (CK1) appear to be mainly involved in the signaling evoked during VSMC activation induced by PDGF-BB. In particular, the modulation of HSP27 and gap junction a-1 protein (connexin 43), seems to be relevant for VSMC phenotype changes. HSP27 has been recently demonstrated to be phosphorylated after PDGF-BB stimulation and to exert a role in VSMC de-differentiation through cytoskeleton remodeling [34].

Connexin 43 is the major protein of gap junctions and it is highly expressed in the neointima during the early stage of arteriosclerosis [35,36]. It has been shown that connexin 43 phosphorylation can regulate the early assembly of functional gap junctional channels [37].

It is also worth discussing the modulation of other proteins such as calreticulin, filamin A (FLNA), PDZ LIM protein 5 and vinculin, since also the modulation of these proteins might be involved in VSMC activation.

Vinculin is a membrane protein that links adhesion molecules to actin cytoskeleton and has a key role in modulating focal adhesion structures and functions thus controlling cell migration. The phosphorylation of Vinculin on tyrosine and serine is well-known and seems to regulate actin filament assembly and cell spreading [38,39,40].

Also the PDZ and LIM domain protein family is involved in focal adhesion assembly [41]. LIM and PDZ domains

may have diverse functions but essentially they provide recognition sites for assembling multiprotein complexes and cytoskeleton. Noteworthy, PDZ-domain-containing proteins serve as scaffolds for assembling complexes involved in cell-cell junctions and signal transduction [42,43]. The extent and role of phosphorylation in modulating the biological functions of these proteins has been poorly investigated.

Caldesmon is an actin-binding protein that plays an essential role in the regulation of cytoskeleton organization modulating VSMC contraction and stabilizing stress fibers and focal adhesions. It has been demonstrated that phosphorylation decreases its actin-binding capacity thereby allowing dynamic changes of actin cytoskeleton that lead to motility and likely activation [44].

Also filamin A is an actin-binding protein and it regulates re-organization of cytoskeleton. It is essential for cell locomotion, interacting with integrins and membrane receptor complexes in VSMCs [45, 46]. Recently, it has been shown that phosphorylated filamin A regulates actin-linked caveolae dynamics [47], moreover, phosphorylation seems to facilitate filamin A binding to integrin suggesting a role, modulated by the degree of phosphorylation, as a mechano-sensor [48].

Calreticulin is an endoplasmic reticulum-resident chaper-

one that binds misfolded proteins and prevents them from being exported, but it is also found in the nucleus and thus may have a role in transcription regulation. More recently, an important role of serine de-phosphorylation and tyrosine phosphorylation on mRNA stability of angiotensin II receptor type 1 (AT1) receptor was investigated [49]. This receptor mediates important biological effects in VSMCs, such as proliferation, vasoconstriction and reactive oxygen species release [50].

It is interesting to underline that up- and down-phosphorylation events are equally represented at early times after stimulation. Probably, once PDGF-BB growth factor binds to its receptor, within a few minutes a cascade of kinases and phosphatases activate a series of biological events and the phosphorylation state of several proteins changes dramatically. As discussed previously, these early events, even if phenotypically imperceptible, are decisive for the activation process in VSMCs [6,10], and the entire reorganization of the cell structure.

4. Concluding Remarks

In summary, we performed for the first time a quantitative phosphoproteome analysis on primary VSMCs in order to investigate biological events induced by PDGF-BB stimulation. Moreover, the SILAC approach applied to VSMC model allowed evaluation of time-course modifications in a quantitative manner. Our approach allowed the identification of 1300 phosphopeptides, one hundred of them resulted novel phospho-sites in pig model, 47 of which are new even in Mouse-Human databases. Furthermore, in VSMC signaling events, some important factors involved in cytoskeleton remodeling, focal adhesions, gap junction assembly and cell activation were found differentially phosphorylated these early phosphorylations, pointed out here for the first time can be considered the starting point for the activation and the reorganization of VSMC.

5. Supplementary material

Supplementary data and information is available at: <http://www.jiomics.com/index.php/jio/rt/suppFiles/126/0>.

Supplementary Material includes Supplementary Tables 1 (List of total identified peptide), 2 (List of

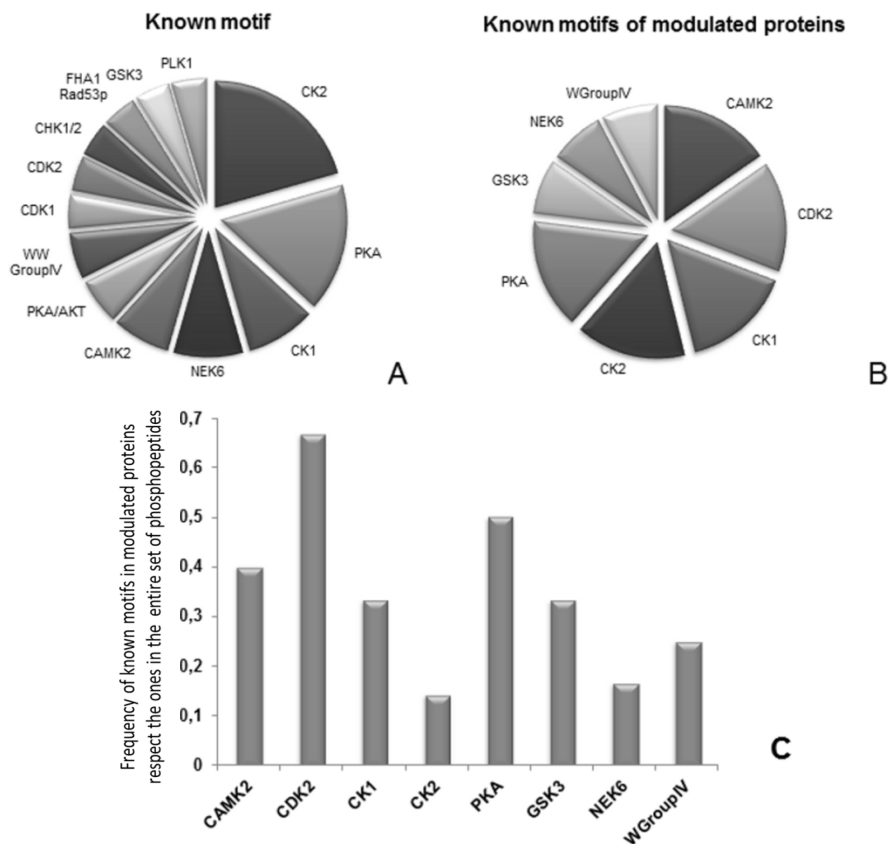


Figure 4. Analysis of the identified phosphopeptides: A: analysis of all identified phosphopeptides. B: analysis of modulated phosphopeptides. C: frequency of known motifs in modulated proteins with respect to the entire list.

total identified groups of proteins) and Supplementary Data (Supplementary Figure 1, 2,3 and Figure 4).

References

1. JD Graves, EG Krebs in: *Pharmacology and Therapeutics* 1999; pp. 111–121.
2. T Hunter, *Cell* (2000) 113–127.
3. G Manning, DB Whyte, R Martinez, T Hunter, S Sudarshanam, *Science* (2002) 1912–1934.
4. Adams MD, Myers EW, Li PW, Mural RJ, Sutton GG, et. al. *Science* (2001) 1304–1351.
5. GK Owens, MS Kumar, BR Wamhoff, *Physiological Reviews* (2004) 767–801.
6. A Cecchetti, S Rocchiccioli, C Boccardi, L Citti, *International review of cell and molecular biology* (2011) 43–99.
7. R Ross, *Nature* (1993) 801–809.
8. WT Gerthoffer, *Circulation Research* (2007) 607–621.
9. C Lande, CBoccardi, L Citti, A Mercatanti, M Rizzo, S Rocchiccioli, L Tedeschi, MG Trivella, A Cecchetti, *BMC Res Notes* (2012) 268 doi:10.1186/1756-0500-5-268.
10. C Boccardi, A Cecchetti, A Caselli, G Camici, M Evangelista, A Mercatanti, G Rainaldi, L Citti, *Cell and tissue research* (2007) 185–95.
11. K Kawai-Kowase, GK Owens, *Am. J. Physiol. Cell Physiol.* (2007) C59–C69 doi: 10.1152/ajpcell.00394.2006.
12. HF Chen, LD Xie, CS Xu, *Mol. Cell. Biochem* (2010) 49–56.
13. C Liu, T Su, F Li, L Li, X Qin, W Pan, F Feng, F Chen, D Liao, L Chen, *Acta Biochim. Biophys. Sin.* (2010) 396–402.
14. PA Suwanabol, SM Seedial, X Shi, F Zhang, D Yamanouchi, D Roenneburg, B Liu, KC Kent, *J Vasc Surg.* (2012) 446–54.
15. Mann M, Ong SE, Gronborg M, Steen H, Jensen ON, Pandey A. Analysis of protein phosphorylation using mass spectrometry: deciphering the phosphoproteome. *Trends Biotechnology* 2002;20: 261–8.
16. LB Areces, V Matafora, A Bachi, *Eur J Mass Spectrom* (Chichester, Eng) (2004) 383–92.
17. B Bodenmiller, R Aebersold, *Methods Enzymol.* (2010) 317–34.
18. SE Ong, B Blagoev, I Kratchmarova, DB Kristensen, H Steen, A Pandey, M Mann, *Molecular and Cellular Proteomics* (2002) 376–86.
19. F Delom, E Chevet, *Proteome Science* (2006) 4:15 doi:10.1186/1477-5956-4-15.
20. GH Han, MI Ye, HF Zou, *Analyst* (2008) 1128–38.
21. A Leitner, *Trends in Analytical Chemistry* (2010) 177–85.
22. F Torta, M Fusi, CS Casari, CE Bottani, A Bachi, *J Proteome Res.* (2009) 1932–42.
23. T Christen, ML Bochaton-Piallat, P Neuville, S Renzen, *Circ Res* (1999) 99–107.
24. V Matafora, A D'Amato, S Mori, F Blasi, A Bachi, *Mol Cell Proteomics* (2009) 2243–55.
25. M. J. Schroeder, J. Shabanowitz, J. C. Schwartz, D. F. Hunt, J. J. Coon, *Anal. Chem* (2004) 3590–8.
26. J. V. Olsen, L. M. de Godoy, G. Li, B. Macek, P. Mortensen, R. Pesch, A. Makarov, O. Lange, S. Horning, M. Mann, *Mol. Cell. Proteomics* (2005) 2010–21.
27. J. V. Olsen, B. Blagoev, F. Gnad, B. Macek, C. Kumar, P. Mortensen, M. Mann, *Cell* (2006) 635–48.
28. S Tine, E Thingholm, ON Jensen, JP Robinson, MR Larsen, *Molecular & Cellular Proteomics* (2008) 661–71.
29. B Boris Macek, I Mijakovic, JV Olsen, F Gnad, C Kumar, PR Jensen, M Mann, *Molecular & Cellular Proteomics* (2007) 697–707.
30. GT Cantin, W Yi, B Lu, SK Park, T Xu, JD Lee, JR Yates III, *Journal of Proteome Research* (2008) 1346–51.
31. B Zhai, J Villén, SA Beausoleil, J Mintseris, SP Gygi, *Journal of Proteome Research* (2008) 1675–82.
32. WX Schulze, M Mann, *Journal of Biological Chemistry* (2004) 10756–64.
33. S Rocchiccioli, L Citti, C Boccardi, N Ucciferri, L Tedeschi, C Lande, MG Trivella, A Cecchetti. *Proteome Science* (2010) 8:15 doi:10.1186/1477-5956-8-15.
34. HF Chen, LD Xie, CS Xu, *Molecular and Cellular Biochemistry* (2010) 49–56.
35. BR Kwak, N Veillard, G Pelli, F Mulhaupt, RW James, *Circulation* (2003) 1033–39.
36. CE Chadjichristos, CM Matter, I Roth, E Sutter, G Pelli, TF Lüscher, M Chanson, BR Kwak, *Circulation* (2006) 2835–43.
37. JL Solan, PD Lampe, *Biochimica et Biophysica Acta* (2005) 154–63.
38. Z Zhang, G Izaguirre, SY Lin, HY Lee, E Schaefer, B Haimovich. *Molecular Biology of the Cell* (2004) 4234–47.
39. K Küpper, N Lang, C Möhl, N Kirchgeßner, S Born, WH Goldmann, R Merkel, B Hoffmann, *Nature* (2010) 171–5.
40. K Küpper, N Lang, C Möhl, N Kirchgeßner, S Born, WH Goldmann, R Merkel, B Hoffmann, *Biochemical and Biophysical Research Communications* (2010) 560–4.
41. N Tamura, K Ohno, T Katayama, N Kanayama, Ko Sat, *Biochemical and Biophysical Research Communications* (2007) 589–94.
42. T Khurana, B Khurana, AA Noegel, *Protoplasma* (2002) 1–12.
43. ZH Baruch, AL Wendell, *Journal of Cell Science* (2001) 3219–31.
44. Q Jiang, R Huang, S Cai, ALA Wang, *Journal of Biomedical Science* (2010) 17:6 doi: 10.1186/1423-0127-17-6
45. N Yu, L Erb, R Shivaji, GA Weisman, CI Seye, *Circulation Research* (2008) 581–8.
46. Y Xu, TA Bismar, J Su, B Xu, G Kristiansen, Z Varga, L Teng, DE Ingber, A Mammoto, R Kumar, MA Alaoui-Jamali, *Journal Expert Medicine* (2010) 2421–37.
47. O Murie, A Echarri, C Hellriegel, DM Pavón, L Beccari, MA Del Pozo, *Journal of Cell Science* (2011) 2763–76.
48. HS Chen, KS Kolahi, MRK Mofrad, *Biophysical Journal* (2009) 3095–04.
49. CFH Mueller, K Wassmann, A Berger, S Holz, S Wassmann, G Nickenig, *Biochemical and Biophysical Research Communications* (2008) 669–74.
50. G Nickenig, DG Harrison, *Circulation* (2002) 393–406.